



Results

1. Evaluation of Physicochemical Characteristics

1.1 Determination of degree of deacetylation of chitosan

1.1.1 Colloidal Titration

Degree of deacetylation of chitosan products was determined and calculated using the method described in Appendix A. Deacetylation of chitin by various reaction time produced chitosan in different degree of deacetylation as shown in Table 8

Table 8 Degree of deacetylation of chitosan products from various reaction time

| Chitosan | Reaction time (hour) | % Deacetylation |
|----------|-------------------------|-----------------|
| CS 2* | 2 | 67.70 |
| CS 3.5 | 3.5 | 71.75 |
| CS 7 | 7 | 72.35 |
| CS 10 | 10 | 78.61 |

* CS was abbreviated from chitosan, the number indicated reaction time using

Chitosan products having different degree of deacetylation were obtained by varying reaction time. It was found that an increasing reaction time could increase degree of deacetylation.

1.1.2 Infrared spectrometry

Infrared spectrometry was employed in this study to determine the residual CONH groups in chitosan products. The IR spectra were depicted in Figure 5 . Each spectra show a peak at about 1700 cm^{-1} for C=O stretching and N-H blending. The majority was from C=O stretching vibration. It was seen that the following spectra were appeared to be similar. From this observation, the absorption peak at about 1700 cm^{-1} in each chitosans associated with the degree of deacetylation measured by colloidal titration except CS2.

1.2 Viscosity measurement

Viscosity of chitosans with different degree of deacetylation was measured and the values of mean and standard deviation are shown in Table 9

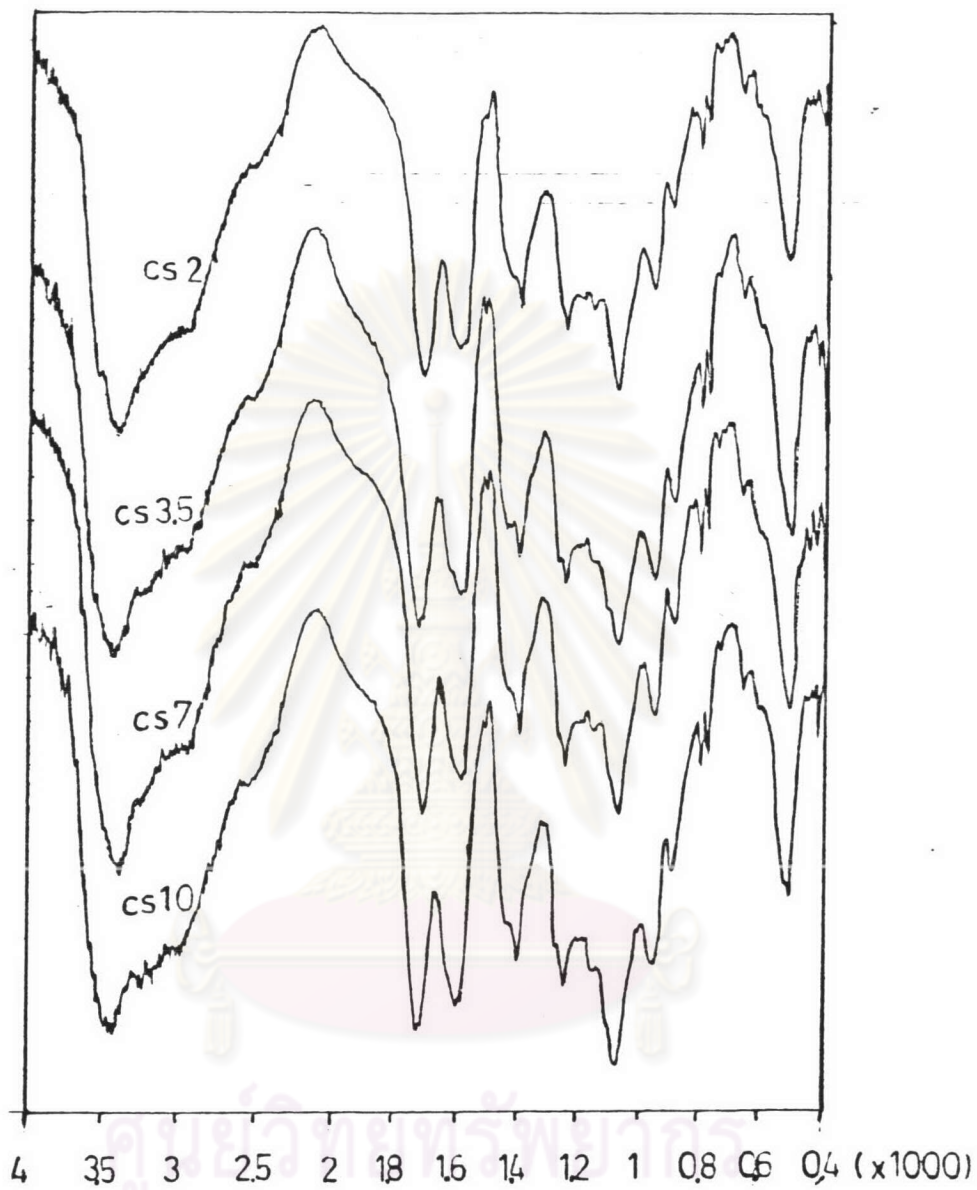


Figure 5 IR spectra of chitosans produced by different reaction time.

Table 9 Viscosity values of 1 % (w/v) chitosan in 2% acetic acid

| Chitosan | Viscosity(cps) \pm s.d. |
|----------|-----------------------------|
| CS 2 | $3.70 \times 10^3 \pm 0.06$ |
| CS 3.5 | $2.65 \times 10^3 \pm 0.16$ |
| CS 7 | $2.47 \times 10^3 \pm 0.16$ |
| CS 10 | 669 ± 10.82 |

The viscosity of chitosan decreased with increasing reaction time. It could be noticed that chitosan having higher degree of deacetylation (chitosan that deacetylated using higher reaction time) exhibited lower viscosity.

2. Evaluation of Physical Properties of Co-Spray Dried Powder

The co-spray dried powder of propranolol hydrochloride and chitosan with various degree of deacetylation were evaluated for their physical properties as follows:

2.1 Morphology of Powder

Figure 6 showed the scanning electron photomicrograph of propranolol hydrochloride powder. Propranolol hydrochloride are varied

in sizes. Each large crystal consisted of small rods.

The photomicrograph of Formulation I-IV were shown in Figure 7-10. The co-spray dried powder of Formulations I-IV exhibited various sizes of microspheres. The surface of microsphere were smooth. The agglomerated particles of Formulation IV were relatively larger than of other formulations. The agglomerated particles of Formulation II were similar to Formulation III.

The photomicrograph of Formulation V-VII were shown in Figure 11-13. The agglomerated particles were consisted of various sizes of microspheres. The agglomerated particles of Formulation V were looser than Formulation VI and VII. The agglomerated particles of Formulation VII were relatively larger than of the other formulations.

2.2 Moisture Determination

The moisture content of co-spray dried powder were reported in Table 10. Each formulations showed similar moisture content in the range 1.60-2.65 % after collection from spray dryer.

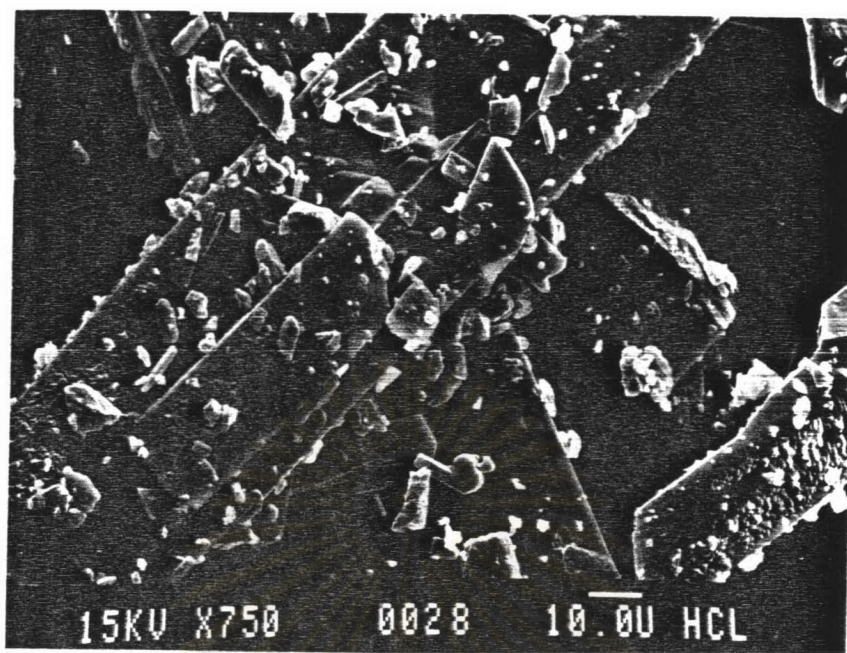


Figure 6 Photomicrograph of Propranolol Hydrochloride

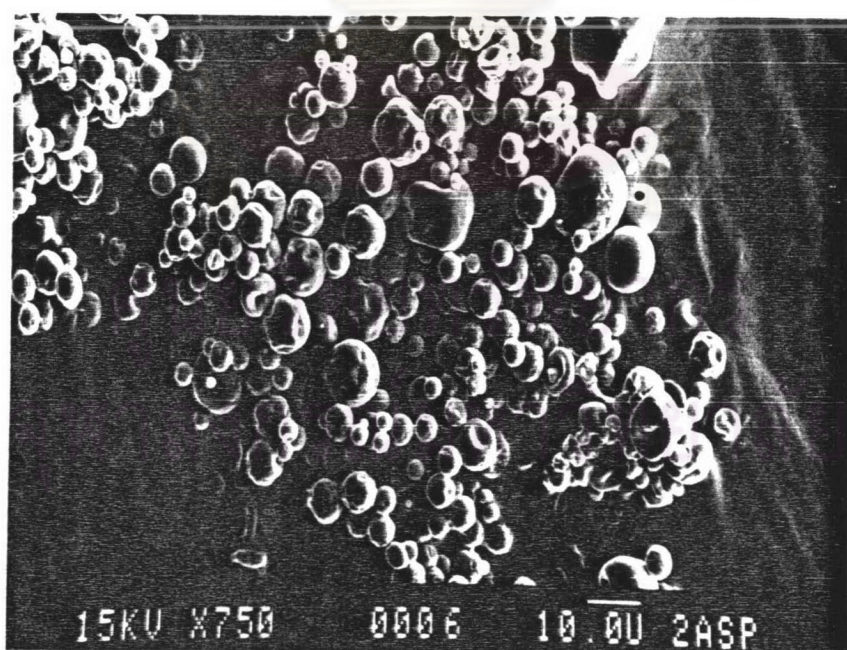


Figure 7 Photomicrograph of co-spray dried of Formulation I

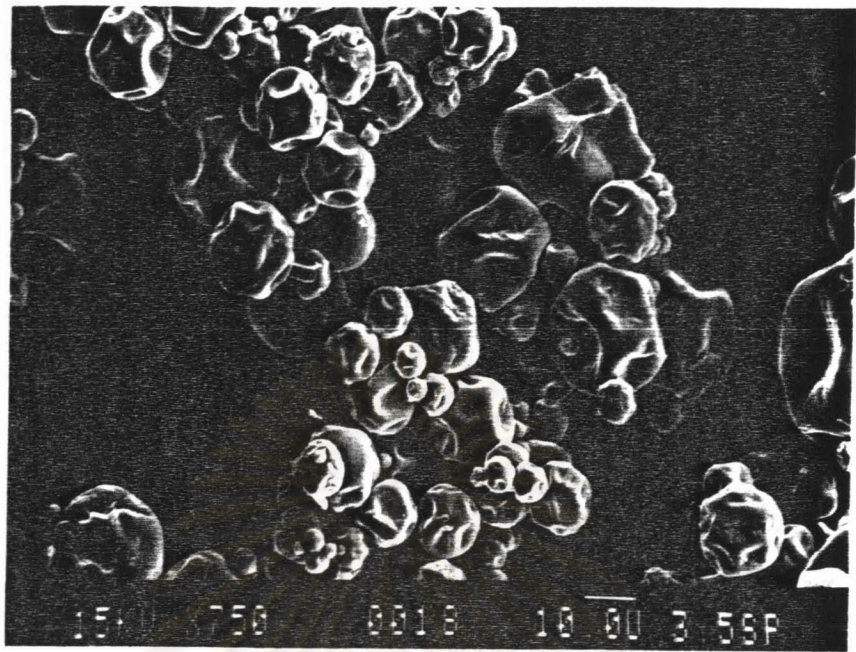


Figure 8 Photomicrograph of co-spray dried of Formulation II

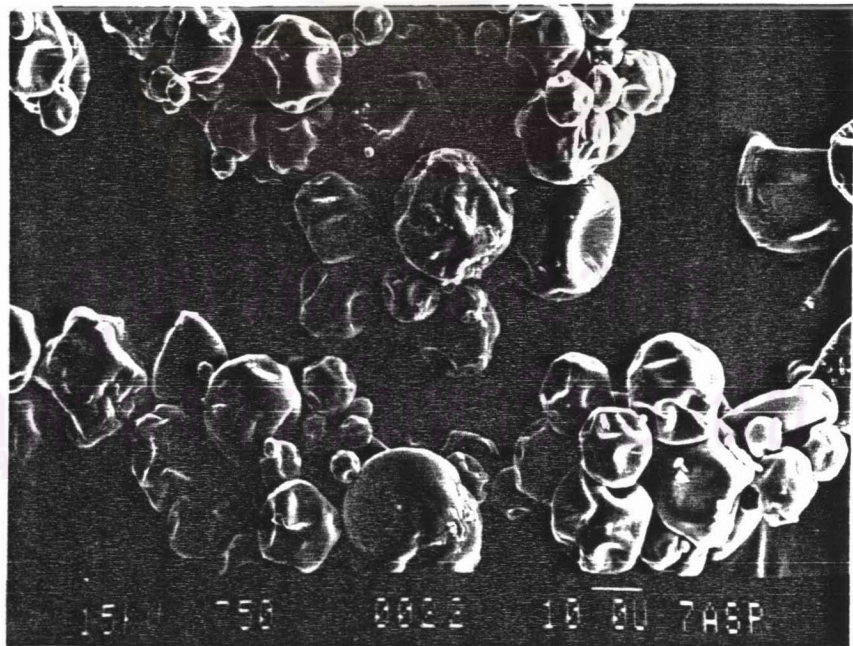


Figure 9 Photomicrograph of co-spray dried of Formulation III.

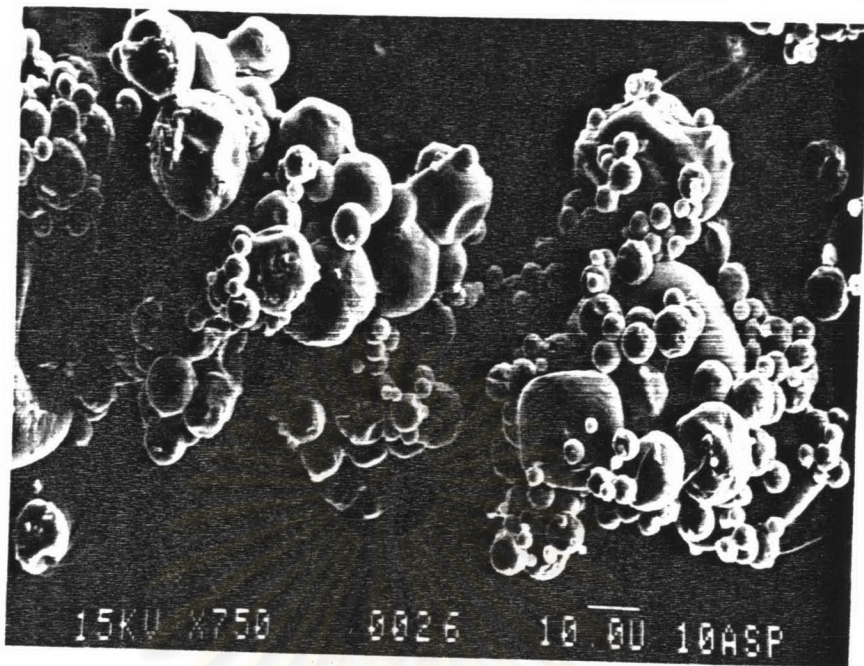


Figure 10 Photomicrograph of co-spray dried of Formulation IV

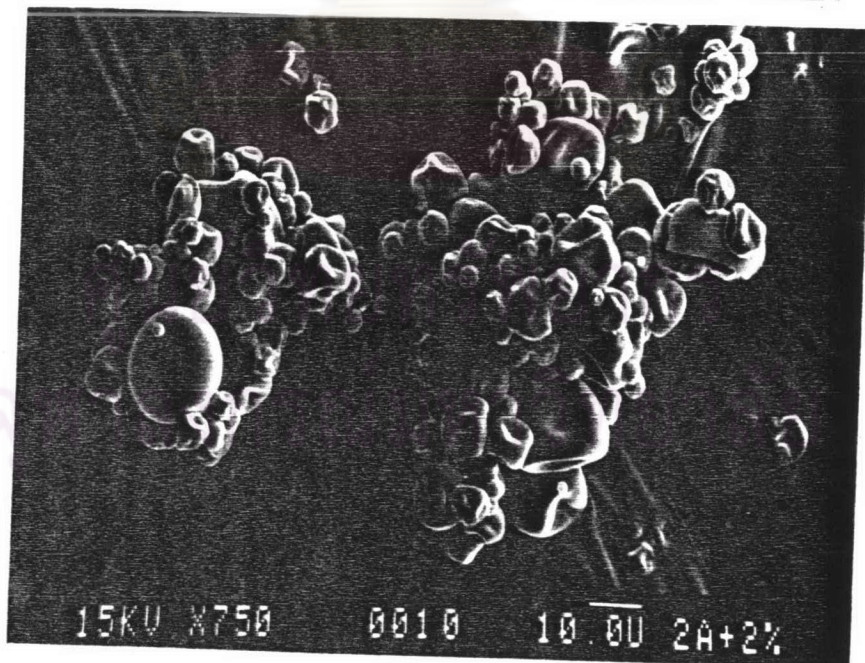


Figure 11 Photomicrograph of co-spray dried of Formulation V.

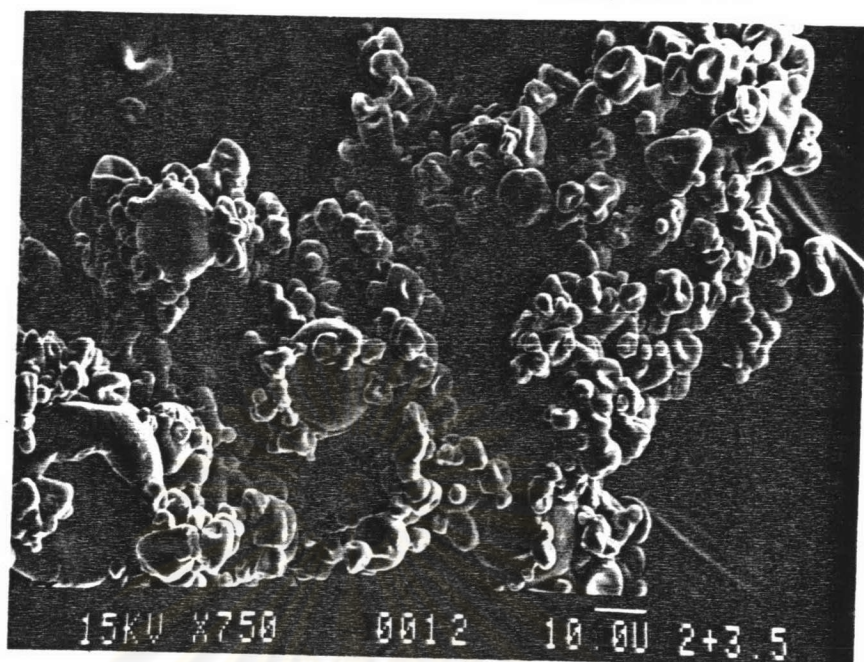


Figure 12 Photomicrograph of co-spray dried of Formulation VI

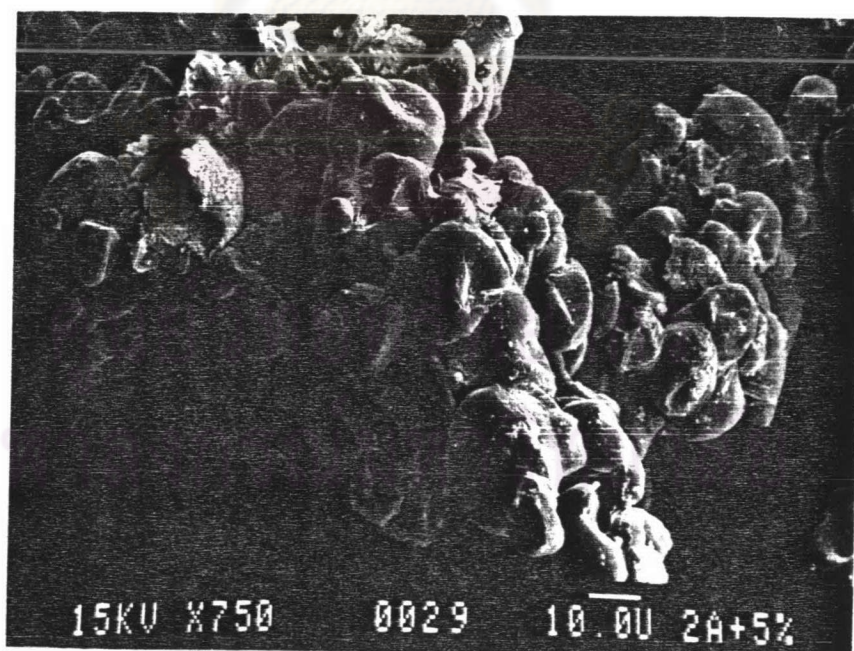


Figure 13 Photomicrograph of co-spray dried of Formulation VII

Table 10 The percentage of moisture content and drug content

| Formulation | % Moisture content \pm s.d. | % Drug content \pm s.d. |
|-------------|-------------------------------|---------------------------|
| I | 2.34 \pm 0.26 | 104.37 \pm 0.27 |
| II | 2.10 \pm 0.21 | 105.78 \pm 0.50 |
| III | 1.95 \pm 0.18 | 105.72 \pm 0.58 |
| IV | 1.80 \pm 0.09 | 102.58 \pm 0.21 |
| V | 2.38 \pm 0.31 | 100.29 \pm 0.60 |
| VI | 2.46 \pm 0.43 | 104.46 \pm 0.50 |
| VII | 2.65 \pm 0.05 | 102.10 \pm 0.37 |

2.3 Drug content

The percent drug content of co-spray dried powder prepared from various formulations were shown in Table 10. Chromatograms from high pressure liquid chromatography were shown in Figures 36-38 (Appendix F). The drug content was in the range 100.29-105.78. The drug was stable in all formulations after collection from spray dryer.

2.4 Particle size distribution

The particle size distribution of co-spray dried powder were shown in Table 11. The particle size distribution was depicted in Figure 34-35 (Appendix c). Formulation II and III showed higher percentage of fine particle than of Formulation I and IV. When

cellulose polymer was added in the Formulation, the particle size of co-spray dried was increased.

Table 11 Particle size distribution of co-spray dried powder

| Preparation | % Weight Retained on Sieve Size(μm) | | | | | |
|-------------|---|-------|-------|-------|-------|-------|
| | 212 | 150 | 106 | 75 | 45 | Pan |
| I | 17.51 | 62.65 | 16.60 | 1.17 | 1.43 | 0.65 |
| II | 12.99 | 8.73 | 12.68 | 43.45 | 17.46 | 4.68 |
| III | 5.82 | 7.15 | 15.12 | 39.84 | 11.44 | 20.53 |
| IV | 11.79 | 6.91 | 55.08 | 10.77 | 12.91 | 2.44 |
| V | 23.50 | 3.20 | 50.70 | 11.70 | 7.50 | 3.40 |
| VI | 22.70 | 17.68 | 53.34 | 4.62 | 0.59 | 1.08 |
| VII | 20.79 | 63.46 | 10.72 | 3.28 | 0.98 | 0.76 |

2.5 X-Ray Diffraction

The X-ray diffraction of propranolol hydrochloride were shown in Figure 14. The diffraction of the original drug shown sharp peak. The X-ray diffraction pattern of propranolol HCl-chitosan (Formulation II) and propranolol HCl-chitosan-HPMC (Formulation V-VII) were shown in Figure 15. In co-spray dried powder of Formulation I and V were in the form of amorphous whereas Formulation VI and VII some of co-spray dried powder were in the form of crystal.

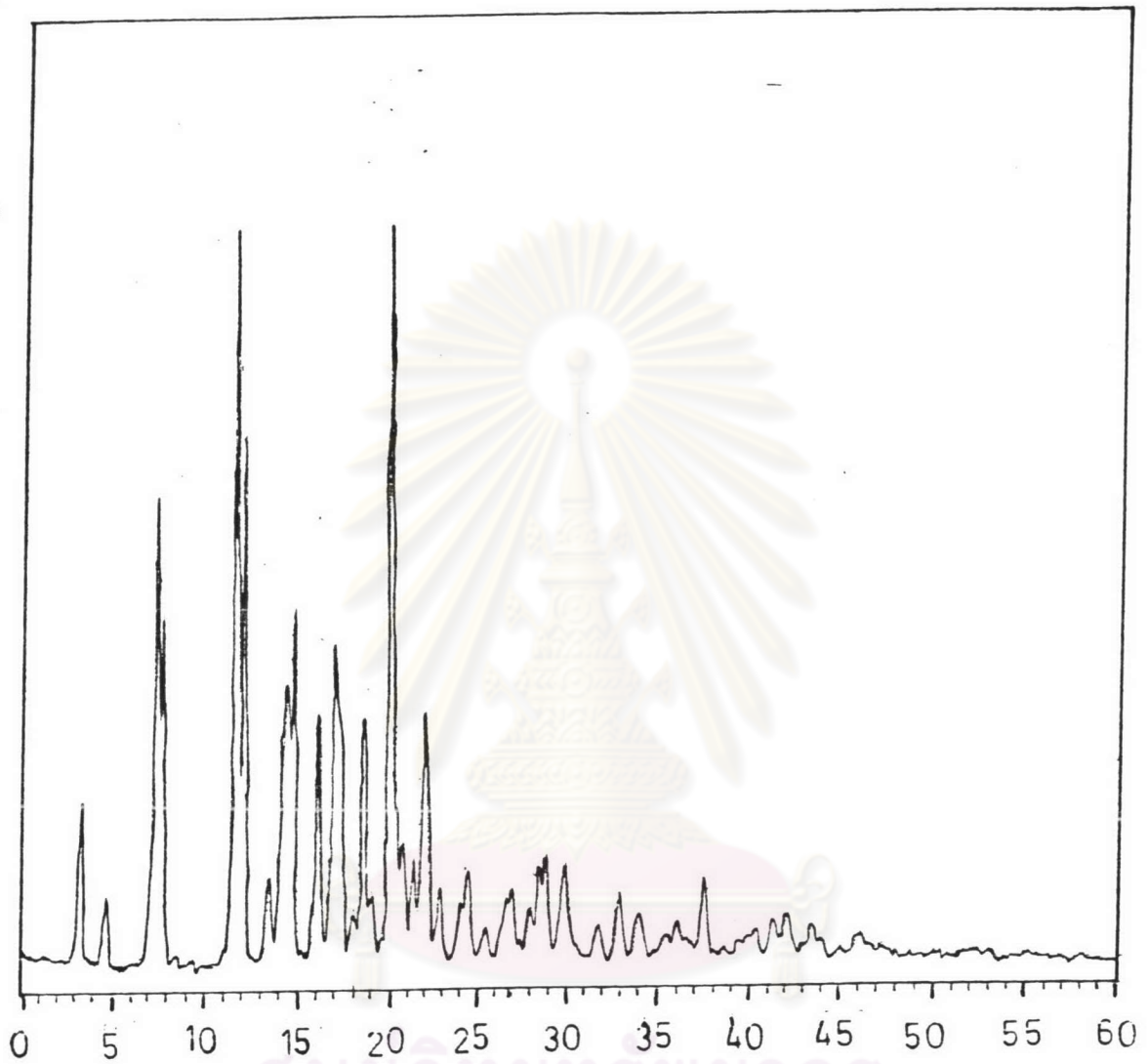


Figure 14 X-ray diffraction spectra of propranolol HCl

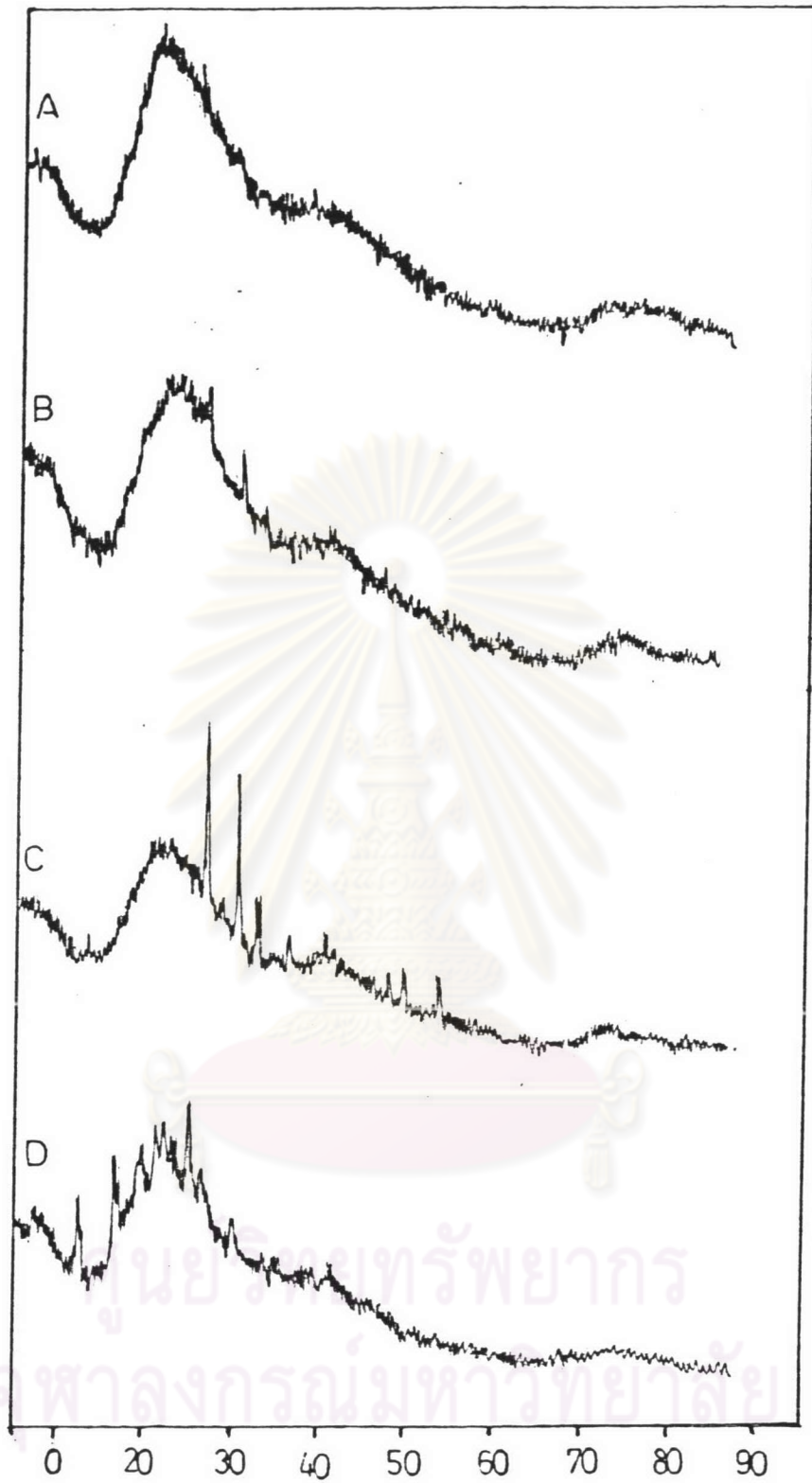


Figure 15 X-ray diffraction spectra of propranolol HCl-chitosan and propranolol HCl-chitosan-HPMC

- A: Propranolol HCl-chitosan (Formulation I)
- B: Propranolol HCl-chitosan-HPMC 2% (Formulation V)
- C: Propranolol HCl-chitosan-HPMC 3.5% (Formulation VI)
- D: Propranolol HCl-chitosan-HPMC 5% (Formulation VII)

3. Evaluation of The Matrix

The co-spray dried powder were compressed into matrices and physical properties were observed.

3.1 Matrix thickness

Although the thickness of matrix tablet was not an official test in quality control of tablet, the uniformity of tablet thickness could predict the uniformity of compression force. The mean and standard deviation of tablet thickness were presented in Table 12. The standard deviations obtained were not exceed 0.03 for all tested matrices.

3.2 Matrix Hardness

The mean and standard deviation of tablet hardness were displayed in Table 12. It was found that the hardness of Formulations I-IV didn't have relationship with reaction time used in deacetylation process. The Formulation I had a lowest hardness value. But incorporating HPMC into the Formulation I caused increases in hardness values. The tablet hardness of Formulation VI-VII were exceed 40 Kp at compression force of 3000 pounds but the hardness the value at compress force 1000 pounds were 14.5 and 15.6, respectively. In this study Formulation VI-VII were compressed at a compression force of 1000 pounds when they were selected to determine the physical property and the release behavior.

3.3 Disintegration study

The means and standard deviations were presented in Table 12. Most of the preparations had disintegration times that were longer than one hour except Formulation IV.

Table 12 Physical Properties of the matrix tablet from different degree of deacetylation of chitosan

| Formulation | Physical Properties of The Matrices | | |
|-------------|-------------------------------------|-----------------------|--------------------------------------|
| | Thickness [mm.±(SD)] | Hardness [Kp±(SD)] | Disintegration Time [minute±(SD)] |
| I | 2.89(0.02) | 2.87(0.14) | 81.02(11.22) |
| II | 2.86(0.03) | 24.67(0.48) | 71.33(3.73) |
| III | 2.85(0.03) | 25.75(1.02) | 61.47(4.62) |
| IV | 2.88(0.02) | 17.93(1.40) | 49.47(4.02) |
| V | 2.82(0.02) | 11.38(0.38) | 87.24(11.25) |
| VI | 2.84(0.02) | >40(14.5=1.05)* | 99.25(8.16) |
| VII | 2.82(0.03) | >40(15.6=0.93)* | 98.02(7.12) |

* the hardness values in parenthesis were obtained at the compression force of 1000 pounds

3.4 Dissolution study

3.4.1 Dissolution Profiles and Release Rate Profile

From the experimental data, the dissolution or the release profiles could be plotted between amount percent of drug release against time. Then, the change of release rate profile was constructed from the dissolution profile to elucidate the release rate at various time interval during the course of drug dissolution from the matrices. The dissolution and release rate profiles of each formulation were described in Table 24-31 (Appendix D).

The release rate was calculated by dividing the difference of percent drug release at various time interval certain amount of the drug (see data in Table 29-31 Appendix D). The rate, then, was plotted with the average time interval. It was shown that the rate of release decreased with the time.

ศูนย์วิทยทรัพยากร
จุฬาลงกรณ์มหาวิทยาลัย

3.4.1.1 Formulations I - IV Matrices

The dissolution profiles of propranolol hydrochloride from propranolol hydrochloride-chitosan matrices with different degree of deacetylation in buffer pH 1.5 and phosphate buffer pH 6.8 were shown in Figure 16(A) (table 24-26 appendix D). Each point represents the average value obtained from six determinations at the given sampling time. The convex curves were turned to the X axis. The release rate was decreased with time as shown in Figure 17(A) and this might be due to an increase in diffusional path length of the drug.

The release of propranolol hydrochloride from matrices containing different degree of deacetylation of chitosan were affected by dissolution medium. Chitosan in Formulation I-III except Formulation IV readily forming a gel at bufferpH 1.5 but showing a poor gel-forming ability at phosphate buffer pH6.8. Increasing degree of deacetylation resulted in a corresponding increase of the dissolution rate in buffer pH 1.5 as displayed in Figure 17(A) whereas the increase of dissolution rate in buffer pH 6.8 did not correspond with the increase degree of deacetylation. Only Formulation I could sustained release until 12 hours both in buffer pH 1.5 and buffer pH 6.8.

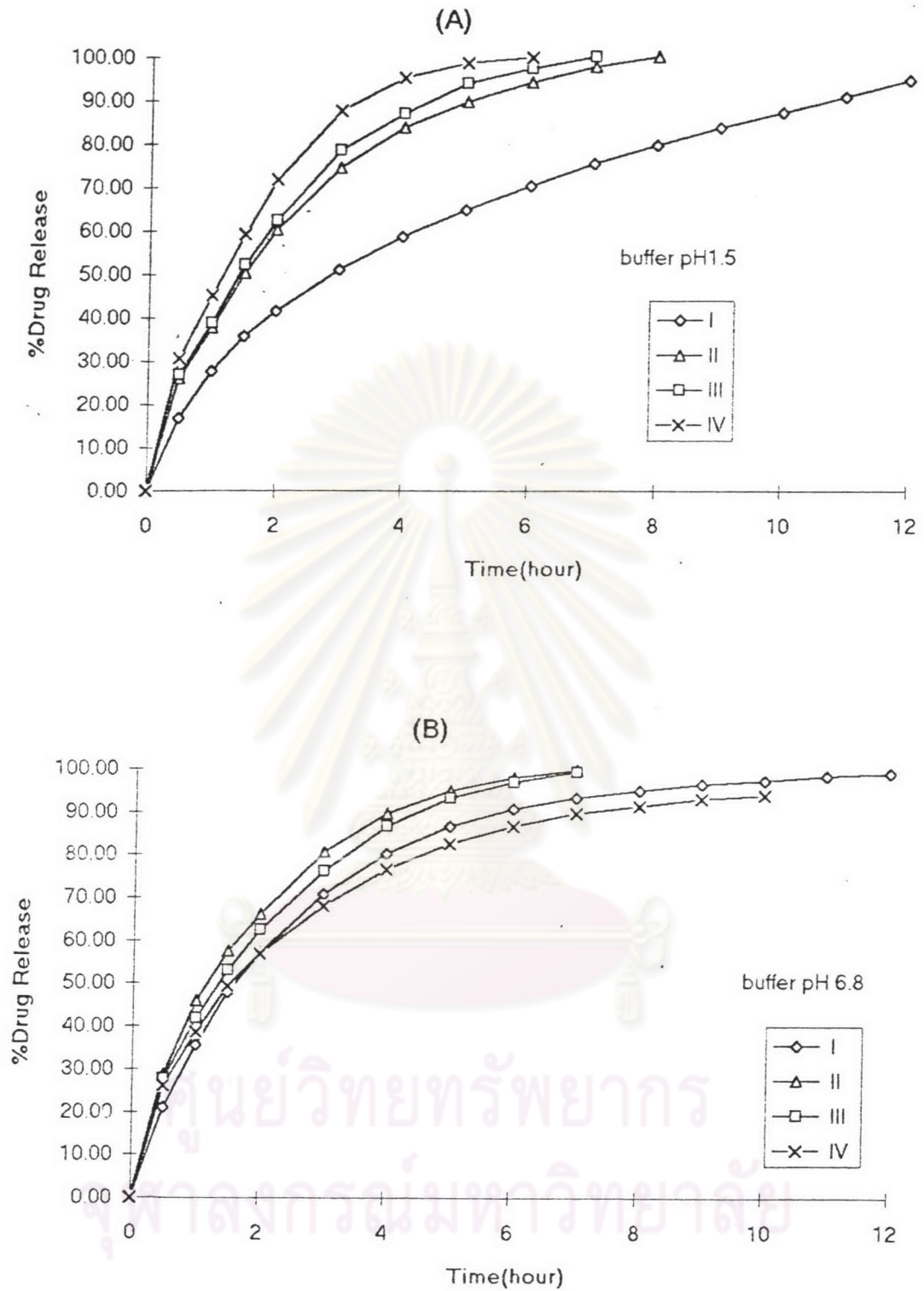


Figure 16 Release profiles of propranolol HCl-chitosan matrices in

A) buffer pH 1.5

B) buffer pH 6.8

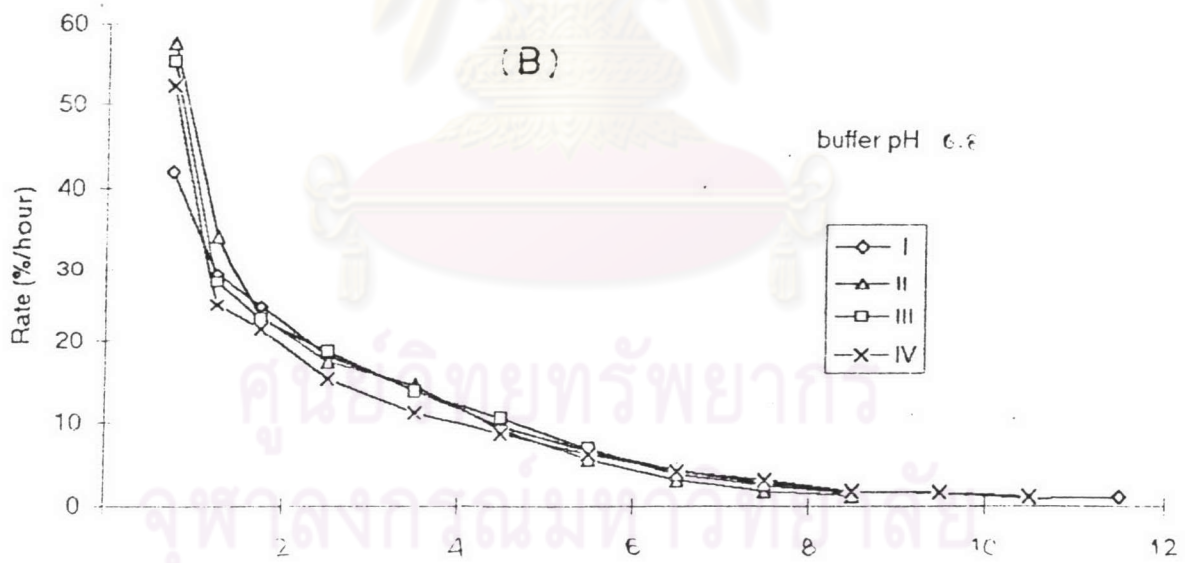
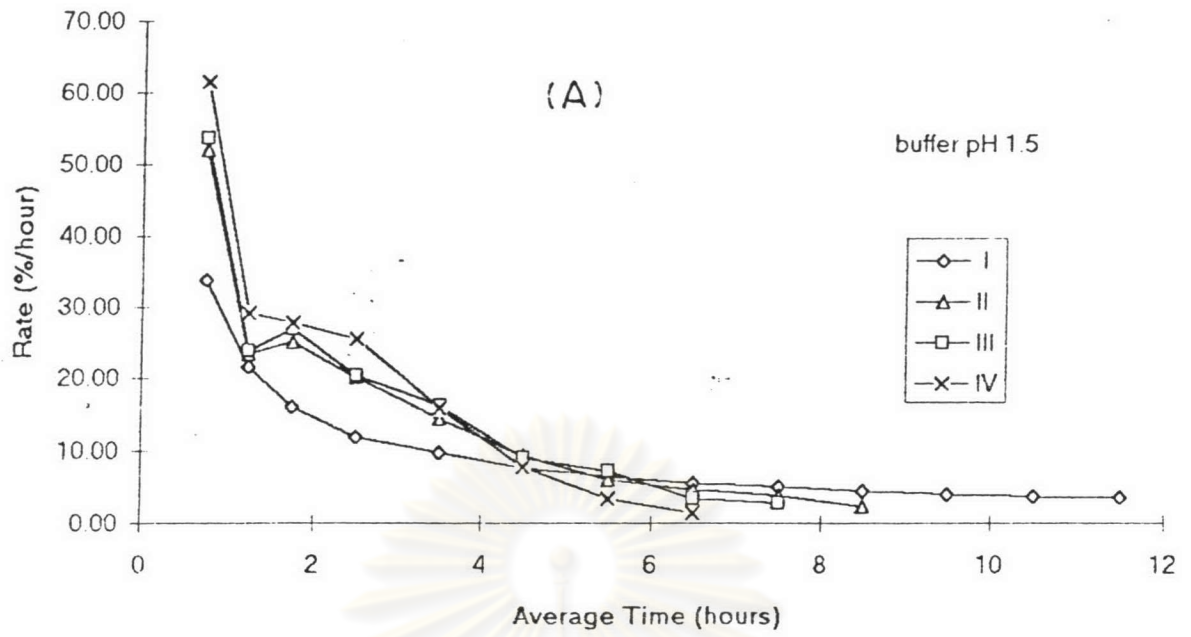


Figure 17 Release rate profiles of propranolol HCl-chitosan matrices in

A) buffer pH 1.5

B) buffer pH 6.8

3.4.1.2 Formulation V-VII Matrices

These formulations contained propranolol HCl -chitosan(CS2)-HPMC but amount of HPMC in each formulations was adjusted differently in order to modify the release rate. In buffer pH 1.5, the dissolution profiles of propranolol hydrochloride from propranolol hydrochloride-HPMC matrices with various amount of HPMC were shown in Figure 18(A) (Table 26, Appendix D). The drug released until 12 hours obtained from formulation VII that had 5% w/w of HPMC. The release rate of this formulation also slower than others as shown in Figure 19(A) (data in Table 29, appendix D). This result may be affected from increase concentration of HPMC. In buffer pH 6.8 the dissolution profiles of formulations V-VII were shown in Figure 18(B) (data in Table 26, Appendix D). The drug released of these formulation obtained until 12 hours. The release rate of formulation V-VII decrease with the time increase as shown in Figure 19(A) and 19(B) (data in table 30, Appendix D).

As these results, it was indicated that the different degree of deacetylation of chitosan affected drug-released time profiles. The pH of medium had an effect on the release rate profile. The concentration of HPMC affected the percentage of drug released.

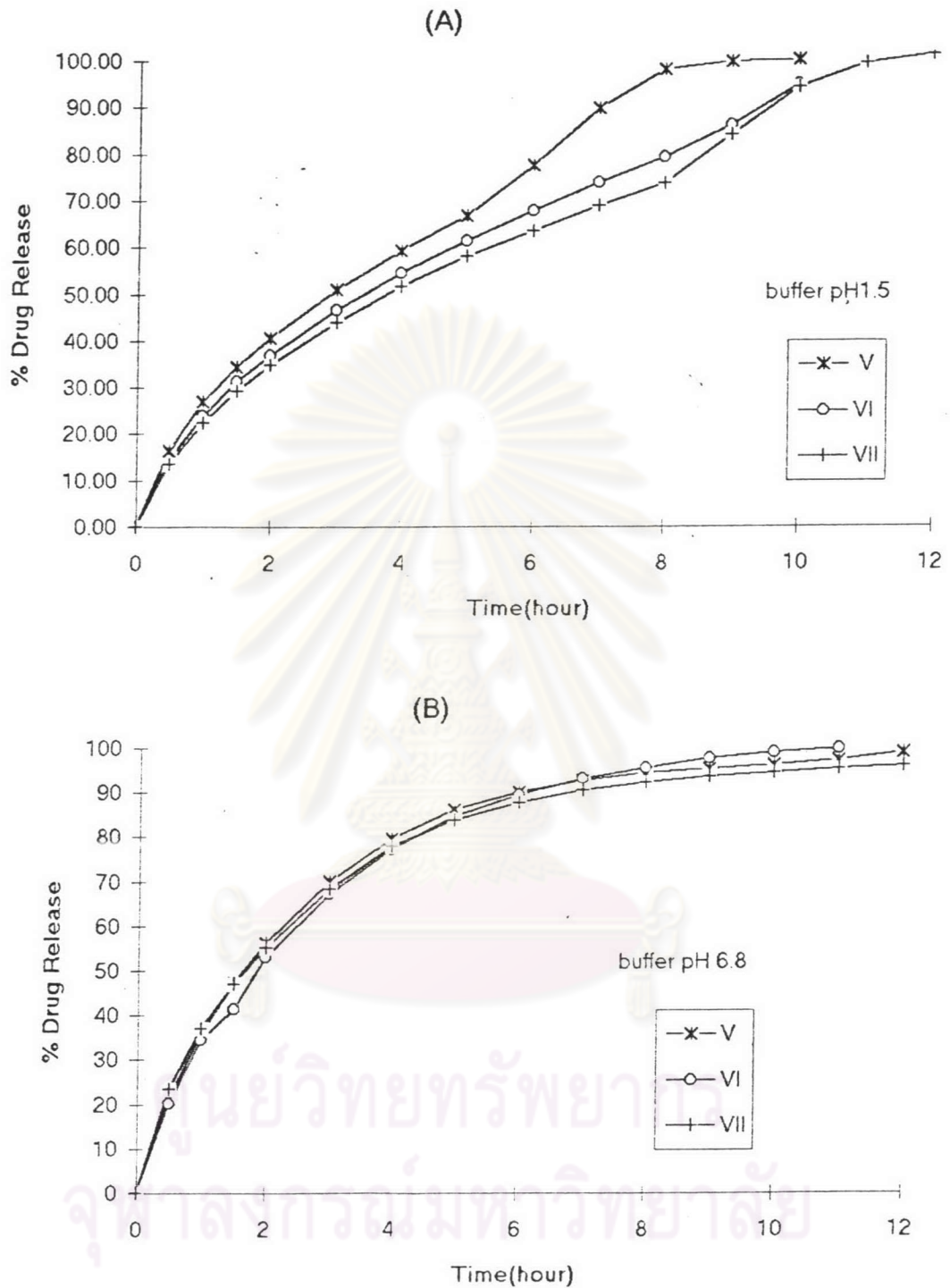


Figure 18 Release profiles of propranolol HCl-chitosan-HPMC

matrices in

A) buffer pH 1.5

B) buffer pH 6.8

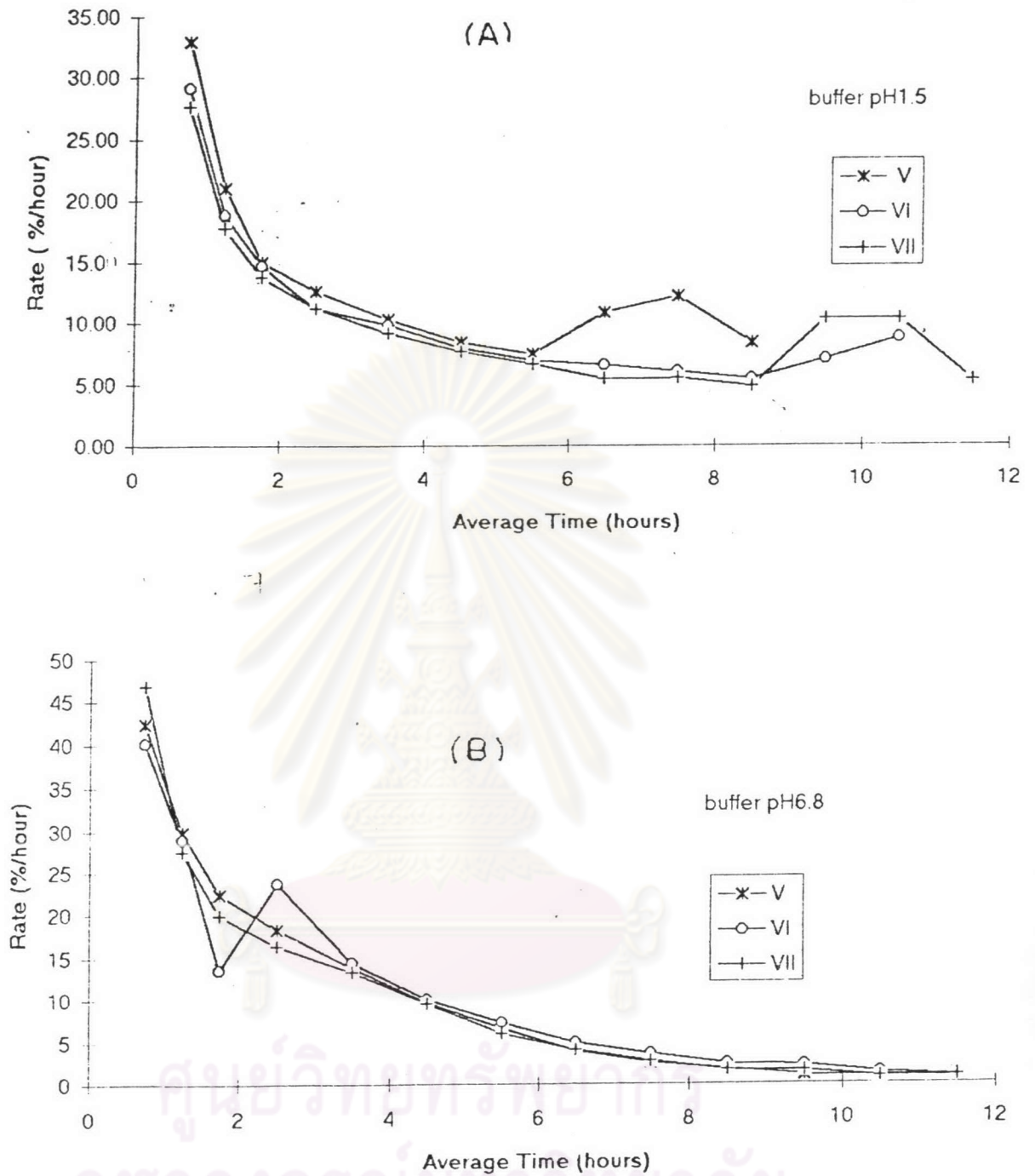


Figure 19 Release rate profiles of propranolol HCl-chitosan-HPMC

matrices in

A) buffer pH 1.5

B) buffer pH 6.8

3.4.1.3 Release studies in pH change method

From the release study as previously described the formulations V, VI, and VII were better than the other formulations. Consequently, these formulations were selected to determine the release behavior by pH change method. The release rate was tested in pH 1.5 for 1.5 hours and then the pH was changed to pH 6.8 run for another 10.5 hours. The drug released and release rate profile were shown in Figure 20 and Figure 21 (Table 27, Appendix D). release characteristics by pH change method according to USP XXIII and compared to the release requirement for propranolol hydrochloride extended release capsule in USP XXIII (Table 32, Appendix D). The drug released and release rate profile attained were presented in Figure 22 and Figure 23, respectively (data in Table 28, Appendix D). The amount of drug released in 6 hours was 81.78% that is slightly higher than requirement in monograph of USP XXIII

3.4.2 Elucidation of Drug Release Model

In order to determine the effect of degree of deacetylation of chitosan and concentration of HPMC on the model of drug release. Therefore, analysis of all dissolution data were carried out to elucidate what model (zero order, first order, Higuchi model) could be fitted by the data. The plots between percentage of drug release versus time (zero order), percentage of drug remained versus time (first order), and percent of drug versus square root of

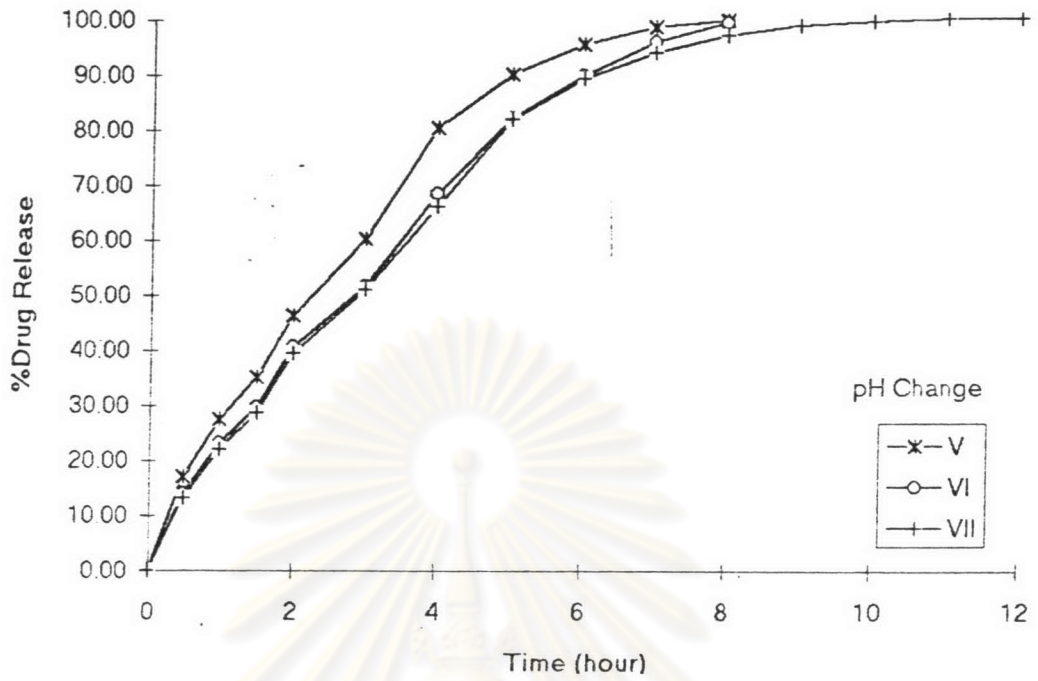


Figure 20 Release profiles of propranolol HCl-chitosan-HPMC matrices in pH change method

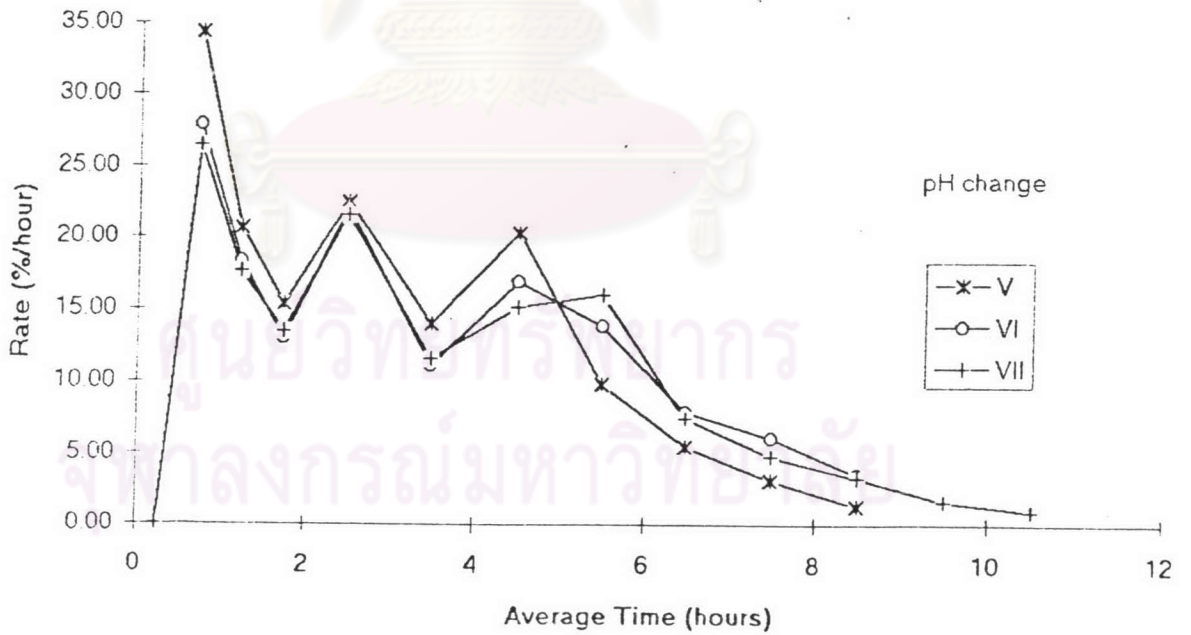


Figure 21 Release rate profiles of propranolol HCl-chitosan-HPMC matrices in pH change method

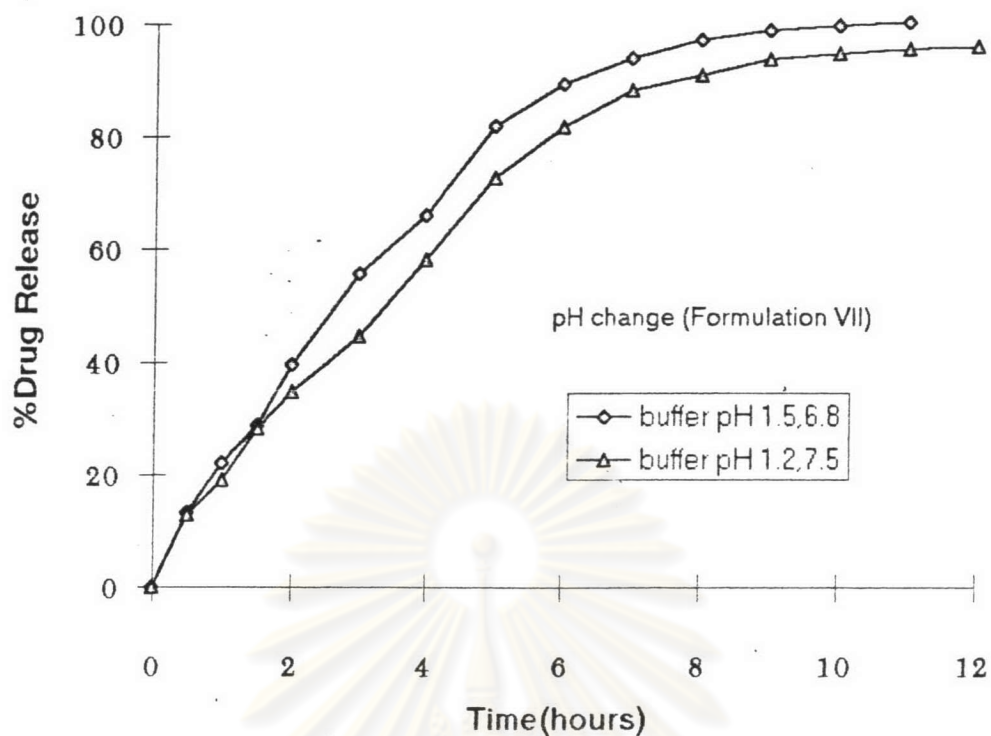


Figure 22 Release profile of Formulation VII
in pH change method

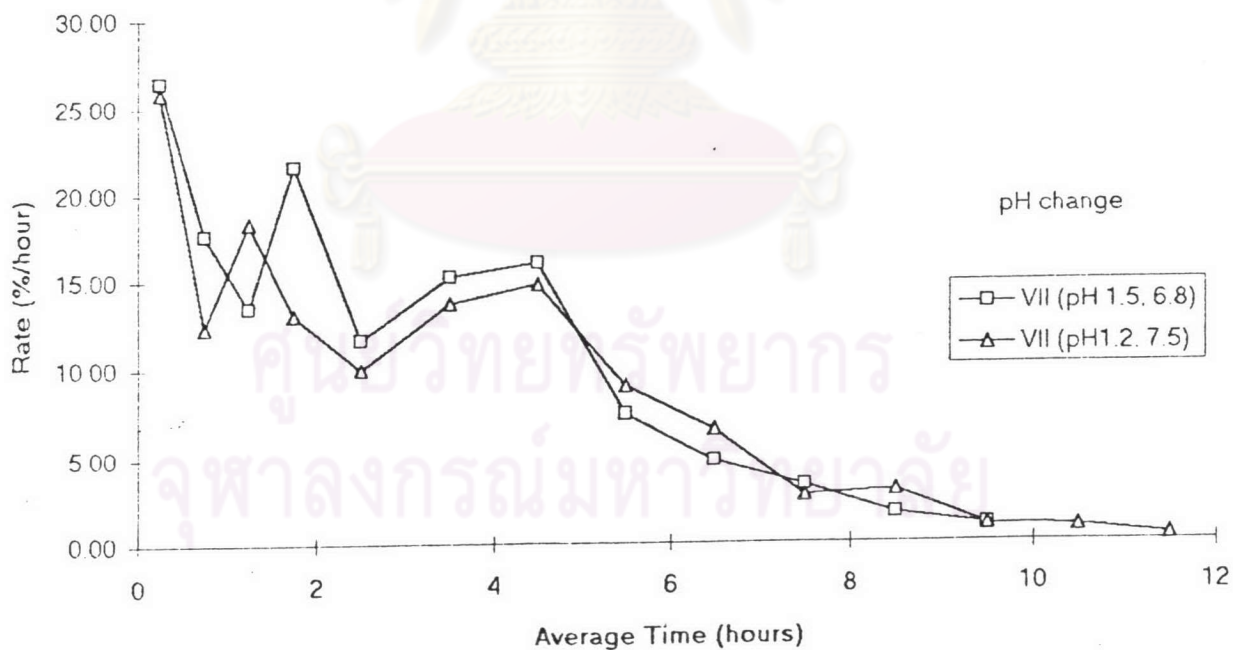


Figure 23 Release rate profile of Formulation VII
in pH change method

time (Higuchi model) were constructed and determined the one which was the most linear and to be the accepted model of drug release.

3.4.2.1 Formulations I-IV Matrices

From the test in buffer pH 1.5, the Higuchi plot and first order plot were shown in Figure 24(A) and Figure 25(A) respectively. From Figures 24(A) and 25(A) the value of correlation coefficients of the relationship shown in Table 13 point out that the first order model and the Higuchi model were interesting. In further treatment, the correlation coefficient of the rates of release against $1/Q$ were higher than those of rates against Q as presented in Table 14. As a result, the Higuchi model would probably be operative.

The Higuchi plot and first-order plot of these formulations in buffer pH 6.8 were shown in Figure 24(B) and Figure 25(B) respectively. From the Figures 24(B) and 25(B), the value of correlation coefficient of the relationship shown in Table 13 pointed out that the first-order model and the Higuchi model were interesting. In further treatment, the correlation coefficients of rates of release against $1/Q$ were higher than those of rate against Q . This was true for Formulation II-IV but Formulation I was opposite as presented in Table 14. The values for the Formulation I showed statistically significant difference (Table 37, Appendix E). The Formulations II-IV would probably follow Higuchi model, while Formulation I would possibly exhibit first-order model.

Table 13 Correlation coefficient of the relationship between percent drug release versus time (A), log percent drug remained versus time (B), percent drug release versus square root time (C)

| Formulation | Correlation coefficient | | | | | |
|-------------|-------------------------|--------|--------|---------------|--------|--------|
| | buffer pH 1.5 | | | buffer pH 6.8 | | |
| | A | B | C | A | B | C |
| I | 0.9080 | 0.9793 | 0.9958 | 0.7641 | 0.9973 | 0.9309 |
| II | 0.8514 | 0.9813 | 0.9789 | 0.7957 | 0.9906 | 0.9576 |
| III | 0.8604 | 0.9875 | 0.9815 | 0.8320 | 0.9900 | 0.9728 |
| IV | 0.8267 | 0.9816 | 0.9697 | 0.7999 | 0.9844 | 0.9579 |
| V | 0.9541 | 0.8355 | 0.9877 | 0.7641 | 0.9848 | 0.9311 |
| VI | 0.9574 | 0.9174 | 0.9944 | 0.8951 | 0.9877 | 0.9540 |
| VII | 0.9702 | 0.8890 | 0.9860 | 0.7637 | 0.9757 | 0.9333 |

Table 14 Comparison of linearity between plots of release against reciprocal amount ($1/Q$) and amount (Q) of propranolol hydrochloride released from the matrices

| Formulation | Correlation coefficient of rate dQ/dt | | | |
|-------------|---|--------------|--------------|--------------|
| | buffer pH1.5 | | buffer pH6.8 | |
| | versus Q | versus $1/Q$ | versus Q | versus $1/Q$ |
| I | 0.8101 | 0.9932 | 0.9887 | 0.8866 |
| II | 0.8717 | 0.9403 | 0.9337 | 0.9764 |
| III | 0.8600 | 0.9104 | 0.9776 | 0.9816 |
| IV | 0.7552 | 0.8219 | 0.8715 | 0.9809 |
| V | 0.6718 | 0.8736 | 0.9814 | 0.9143 |
| VI | 0.6548 | 0.9665 | 0.9357 | 0.8670 |
| VII | 0.5677 | 0.8865 | 0.9010 | 0.9746 |

ศูนย์วิทยทรัพยากร
จุฬาลงกรณ์มหาวิทยาลัย

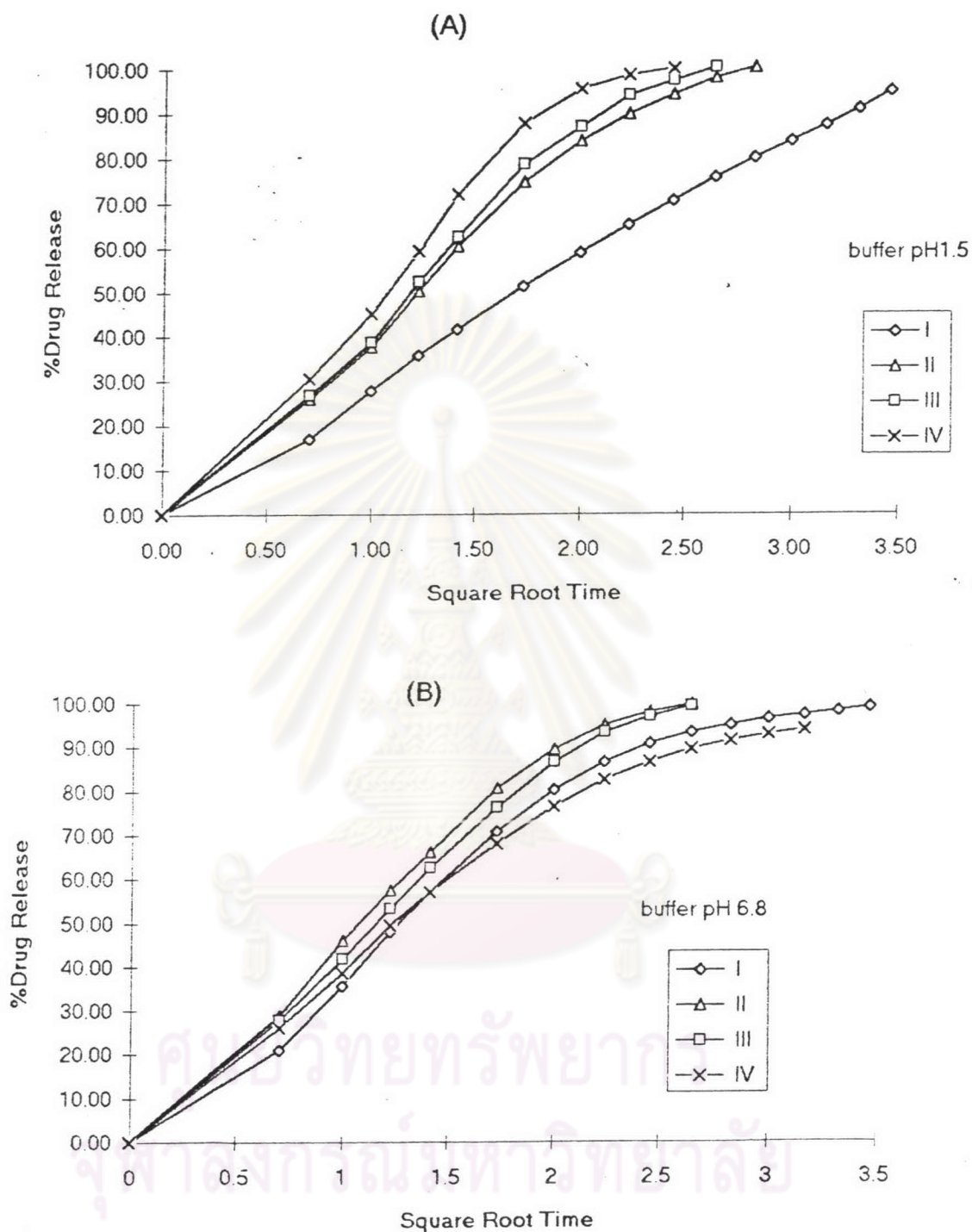


Figure 24 Higuchi plot of Propranolol HCl-chitosan matrices in

A) buffer pH 1.5

B) buffer pH 6.8

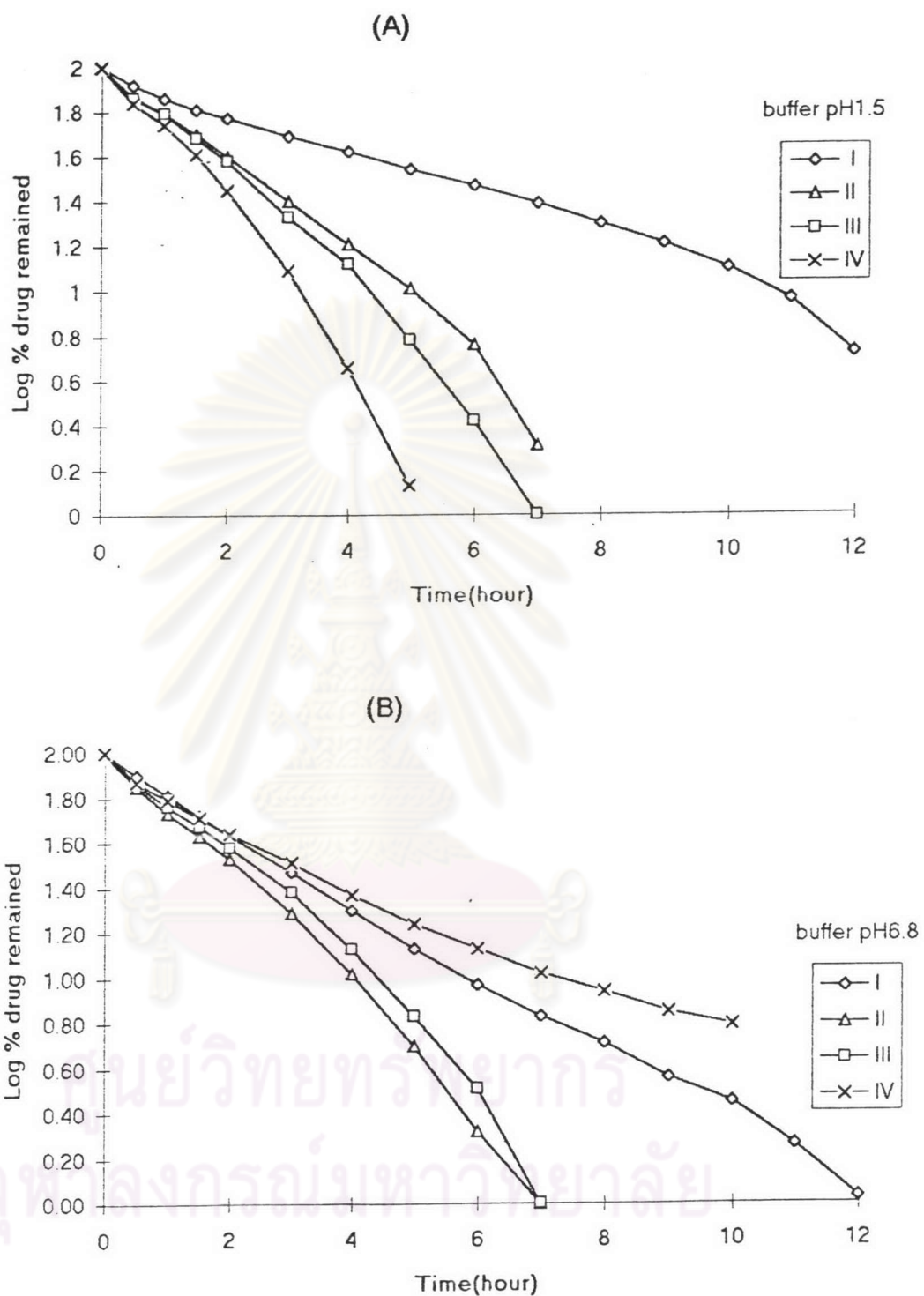


Figure 25 First-order plot of propranolol HCl-chitosan

matrices in

A) buffer pH 1.5

B) buffer pH 6.8

3.4.2.2 Formulations V-VII Matrices

The Higuchi plots and first-order plots were shown in Figures 26 and 27, respectively. In buffer pH 1.5, the highest correlation coefficients were 0.9877, 0.9946 and 0.9859 for Formulation V, VI and VII, respectively that obtained from Higuchi plot (Table 13). In further treatment, the release profile of Formulation V-VII in buffer pH 1.5 would probably follow Higuchi model with correlation coefficient of rate of release against $1/Q$ was higher than that of rate against Q as tabulated in table 14. In buffer pH 6.8, the Higuchi plot and first-order plot were shown in Figure 26 (B) and 27(B) respectively. From the Figure 26(B) and 27(B) the values of correlation coefficient of the relationship shown in Table 13 pointed out that the first order and the Higuchi model were interested. In further treatment, the correlation coefficient of rate of release against Q were higher than those of rates against $1/Q$. This was true for Formulation V-VI but Formulation VII showed opposite results as shown in Table 14. The statistically significant difference of Formulations V-VII were observed, but the t-value of Formulation VI and VII showed no statistically significant difference (Table 37, Appendix E). Therefore, the release profile of Formulation V would probably follow first-order model, while the model of Formulation VI -VII were unclear.

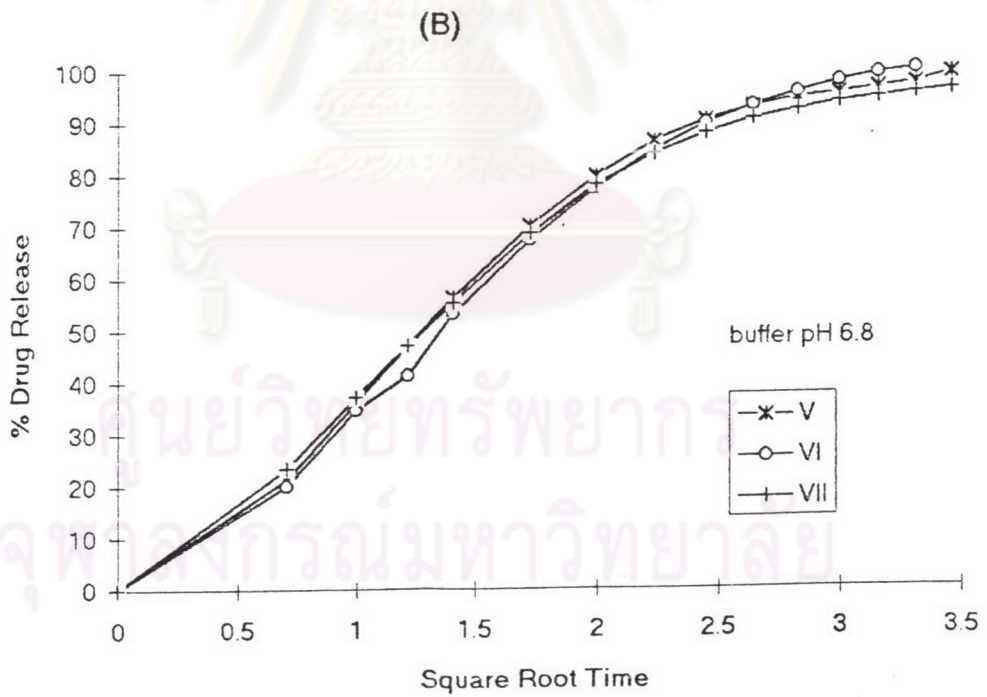
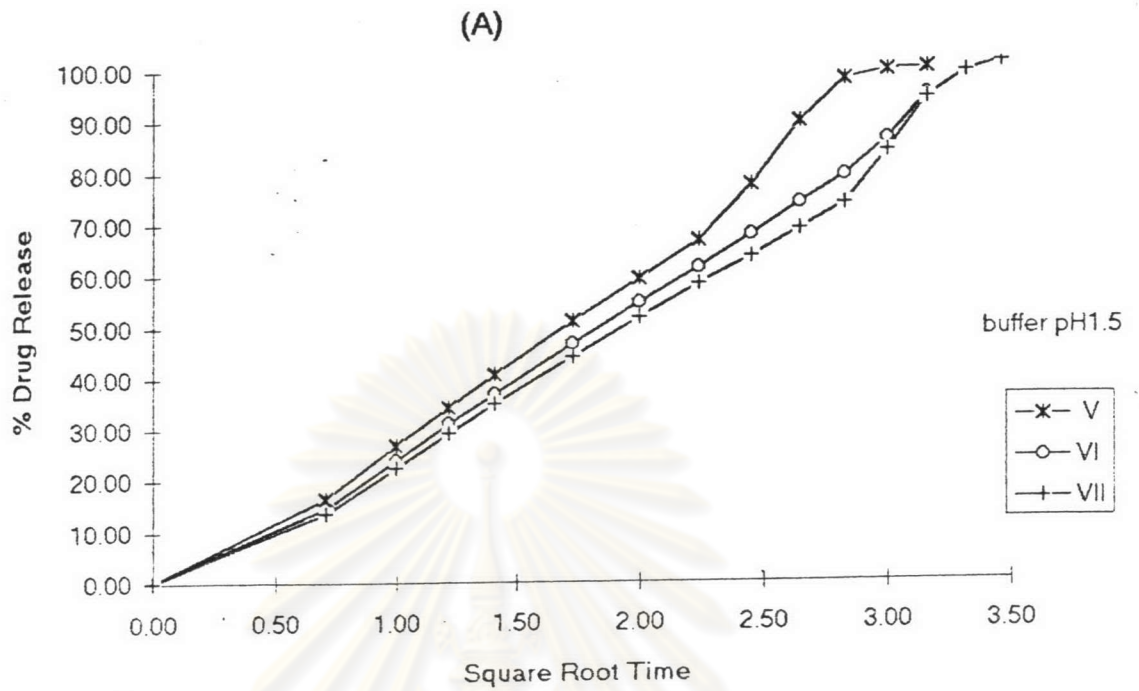


Figure 26 Higuchi plot of Propranolol HCl-chitosan-HPMC

matrices in

A) buffer pH 1.5

B) buffer pH 6.8

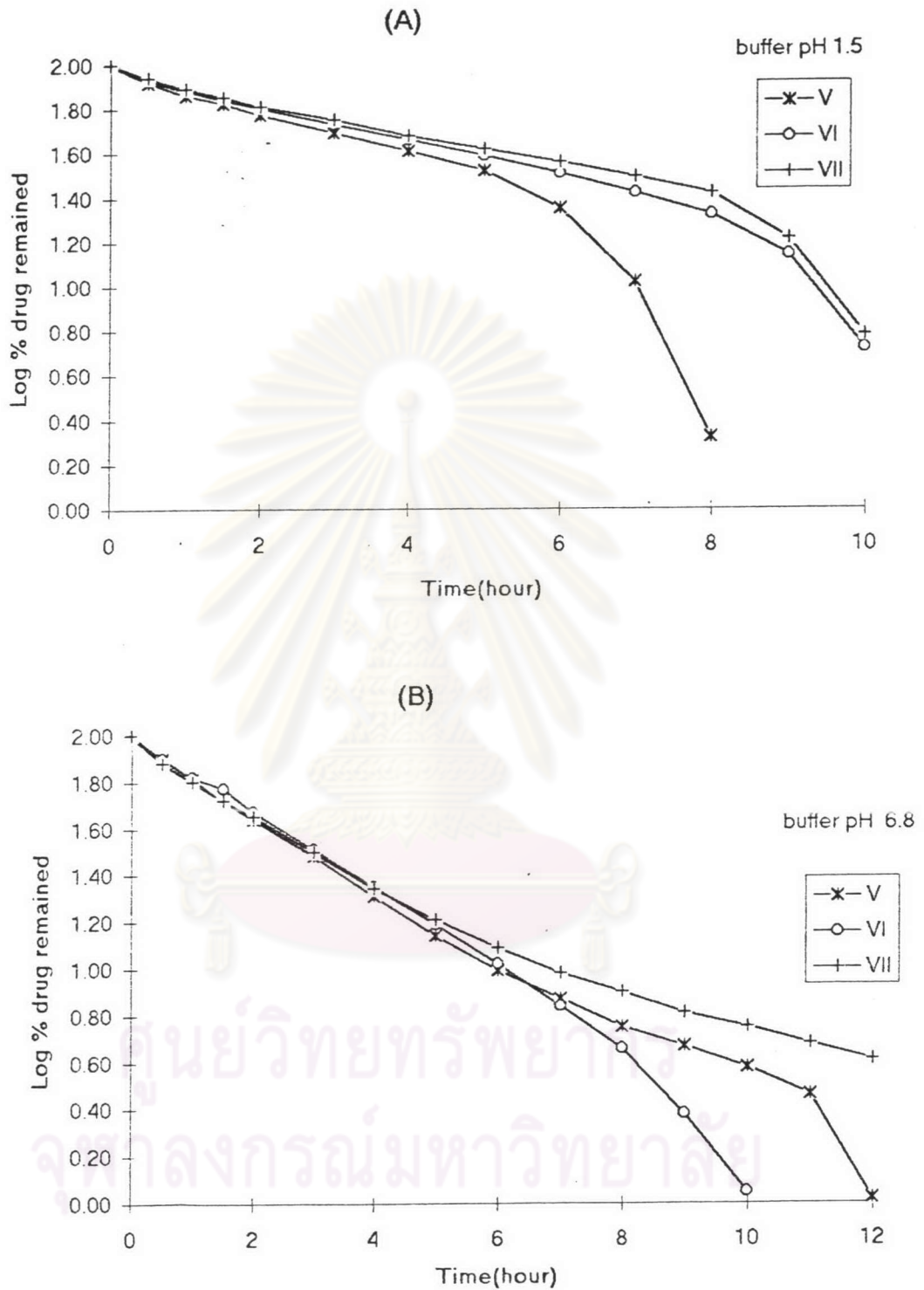


Figure 27 First-order plot of propranolol HCl-chitosan-HPMC matrices in

A) buffer pH 1.5

B) buffer pH 6.8

3.4.2.3 Formulation V-VII in pH Change Method

The Higuchi plots and first-order plots were shown in Figures 28-31. Table 15 showed that the first-order model and Higuchi model were interesting. In further evaluation the correlation coefficient value of rate versus Q was higher than that the rate versus $1/Q$ as shown in Table 16 and indicated that first-order model would probably be operative in Formulations V-VII.

3.4.3 The Evaluation of Drug Release Mechanism

The dissolution data was analyzed to clarify drug release mechanism using equation $M_t/M_\infty = kt^n$ ($M_t/M_\infty < 0.6$) as previously discussed in the section of the analysis of drug release mechanism. The computer program (Leesawat, 1991) was employed. The release exponent (n), kinetic constant (k) and correlation coefficient (r^2) were shown in Table 17-19.

The propranolol hydrochloride-chitosan and propranolol hydrochloride-chitosan-HPMC matrices would be separated the evaluation into two parts according to the characteristics in dissolution medium. In buffer pH 1.5, most of the formulation were formed a gelatinous matrix and swelled. The release exponent value would be compared with the value of cylindrical sample in Table 2. The release mechanism was anomalous (non Fickian) transport. In buffer pH 6.8, Formulation I-VII were not formed a gelatinous matrix and swelled. The release exponent

value would be compared with the value of cylindrical sample in Table 3. The release mechanism was anomalous (non-Fickian) transport.



ศูนย์วิจัยทรัพยากร
จุฬาลงกรณ์มหาวิทยาลัย

Table 15 Correlation coefficient of the relationship between percent drug release versus time (A), log percent drug remained versus time (B), percent drug release versus square root time (C) in pH change method

| Fomulation | A | B | C |
|---------------|--------|--------|--------|
| V | 0.9231 | 0.9448 | 0.9748 |
| VI | 0.9641 | 0.9241 | 0.9743 |
| VII | 0.9537 | 0.8940 | 0.9659 |
| VII(1.2, 7.5) | 0.8960 | 0.9864 | 0.9672 |

Table 16 Comparison of linearity between plots of release against reciprocal amount ($1/Q$) and amount (Q) of propranolol hydrochloride released from the matrices from pH change method

| Formulation | Correlation Coefficient of Rate dQ/dt | |
|---------------|---|--------------|
| | versus Q | versus $1/Q$ |
| V | 0.7330 | 0.7070 |
| VI | 0.7203 | 0.6381 |
| VII | 0.7676 | 0.5998 |
| VII(1.2, 7.5) | 0.7483 | 0.6414 |

ศูนย์วิทยทรัพยากร
จุฬาลงกรณ์มหาวิทยาลัย

Table 17 The value of kinetic constant (k) release exponent (n) and correlation coefficient (r²) following linear regression of dissolution data for values of Mt/Mo in pH 1.5

| Formulation | n (release exponent) | k (kinetic constant) | r ² (coefficient of correlation) |
|-------------|-------------------------|-------------------------|--|
| I | 0.56 | 0.275 | 0.9941 |
| II | 0.61 | 0.387 | 0.9938 |
| III | 0.62 | 0.400 | 0.9915 |
| IV | 0.61 | 0.459 | 0.9974 |
| V | 0.59 | 0.265 | 0.9975 |
| VI | 0.60 | 0.224 | 0.9976 |
| VII | 0.60 | 0.239 | 0.9966 |

Table 18 The value of kinetic constant (k) release exponent (n) and correlation coefficient (r²) following linear regression of dissolution data for values of Mt/Mo in pH 6.8

| Formulation | n (release exponent) | k (kinetic constant) | r ² (coefficient of correlation) |
|-------------|-------------------------|-------------------------|--|
| I | 0.71 | 0.35 | 0.9975 |
| II | 0.61 | 0.39 | 0.9938 |
| III | 0.59 | 0.42 | 0.9999 |
| IV | 0.56 | 0.39 | 0.9990 |
| V | 0.69 | 0.35 | 0.9965 |
| VI | 0.60 | 0.37 | 0.9982 |
| VII | 0.64 | 0.38 | 0.9229 |

Table 19 The value of kinetic constant (k) release exponent (n) and correlation coefficient (r²) following linear regression of dissolution data for values of Mt/Mo in pH change method

| Formulation | n (release exponent) | k (kinetic constant) | r ² (coefficient of correlation) |
|---------------|-------------------------|-------------------------|--|
| V | 0.73 | 0.2731 | 0.9909 |
| VI | 0.74 | 0.2309 | 0.9923 |
| VII | 0.77 | 0.2210 | 0.9935 |
| VII(1.2, 7.5) | 0.82 | 0.1750 | 0.9966 |

Table33 Value for rate, amount release, and the corresponding reciprocal for the release of Formulations I-IV

| Formulation | Dissolution medium | | | | | |
|-------------|--------------------|--------|-------|--------------|-------|-------|
| | buffer pH1.5 | | | buffer pH6.8 | | |
| | dQ/dt | Q | 1/Q | dQ/dt | Q | 1/Q |
| I | 33.76 | 16.88 | 0.059 | 41.86 | 20.93 | 0.048 |
| | 21.64 | 27.70 | 0.036 | 29.32 | 35.59 | 0.028 |
| | 15.98 | 35.69 | 0.028 | 24.48 | 47.83 | 0.02 |
| | 11.72 | 41.55 | 0.024 | 18.06 | 56.86 | 0.018 |
| | 9.61 | 51.16 | 0.02 | 13.70 | 70.56 | 0.014 |
| | 7.51 | 58.67 | 0.017 | 9.47 | 80.03 | 0.012 |
| | 6.27 | 64.94 | 0.015 | 6.49 | 86.52 | 0.012 |
| | 5.50 | 70.44 | 0.014 | 4.09 | 90.61 | 0.011 |
| | 5.05 | 75.49 | 0.013 | 2.62 | 93.23 | 0.011 |
| | 4.40 | 79.89 | 0.012 | 1.67 | 94.90 | 0.01 |
| | 3.89 | 83.78 | 0.012 | 1.46 | 96.36 | 0.01 |
| | 3.55 | 87.33 | 0.011 | 0.81 | 97.17 | 0.01 |
| | 3.44 | 92.77 | 0.011 | 1.01 | 98.18 | 0.01 |
| | 3.91 | 94.68 | 0.01 | 0.74 | 98.92 | 0.01 |
| II | 51.90 | 25.95 | 0.038 | 57.50 | 28.75 | 0.035 |
| | 23.38 | 37.64 | 0.026 | 34.12 | 45.81 | 0.022 |
| | 25.00 | 50.14 | 0.02 | 23.06 | 57.34 | 0.017 |
| | 20.14 | 60.21 | 0.017 | 17.30 | 65.99 | 0.015 |
| | 14.35 | 74.56 | 0.013 | 14.53 | 80.52 | 0.012 |
| | 9.26 | 83.82 | 0.012 | 8.99 | 89.51 | 0.011 |
| | 5.90 | 89.72 | 0.011 | 5.42 | 94.93 | 0.01 |
| | 4.52 | 94.24 | 0.011 | 2.99 | 97.92 | 0.01 |
| | 3.70 | 97.94 | 0.01 | 1.73 | 99.65 | 0.01 |
| | 2.32 | 100.26 | 0.01 | | | |
| III | 53.52 | 26.76 | 0.037 | 56.20 | 27.60 | 0.036 |
| | 23.84 | 38.68 | 0.026 | 28.12 | 41.66 | 0.024 |
| | 26.84 | 52.10 | 0.019 | 22.60 | 52.96 | 0.019 |
| | 20.83 | 62.29 | 0.016 | 18.68 | 62.30 | 0.016 |
| | 16.21 | 78.50 | 0.013 | 13.72 | 76.02 | 0.013 |
| | 8.44 | 86.94 | 0.012 | 10.49 | 86.51 | 0.012 |
| | 7.07 | 94.01 | 0.011 | 6.69 | 93.20 | 0.011 |
| | 3.35 | 97.36 | 0.01 | 3.57 | 96.77 | 0.01 |
| | 2.78 | 100.14 | 0.01 | 2.31 | 99.08 | 0.01 |
| | | | | | | |
| IV | 90.32 | 45.16 | 0.022 | 52.20 | 26.10 | 0.038 |
| | 27.78 | 59.05 | 0.017 | 24.68 | 38.44 | 0.026 |
| | 25.46 | 71.78 | 0.014 | 21.44 | 49.16 | 0.02 |
| | 31.72 | 87.64 | 0.011 | 15.22 | 56.77 | 0.018 |
| | 7.75 | 95.39 | 0.01 | 11.06 | 67.83 | 0.015 |
| | 3.25 | 98.64 | 0.01 | 8.54 | 76.37 | 0.013 |
| | 1.38 | 100.02 | 0.01 | 6.11 | 82.48 | 0.012 |
| | | | | 4.03 | 86.51 | 0.012 |
| | | | | 3.00 | 89.51 | 0.011 |
| | | | | 1.73 | 91.24 | 0.011 |
| | | | 1.61 | 92.85 | 0.011 | |

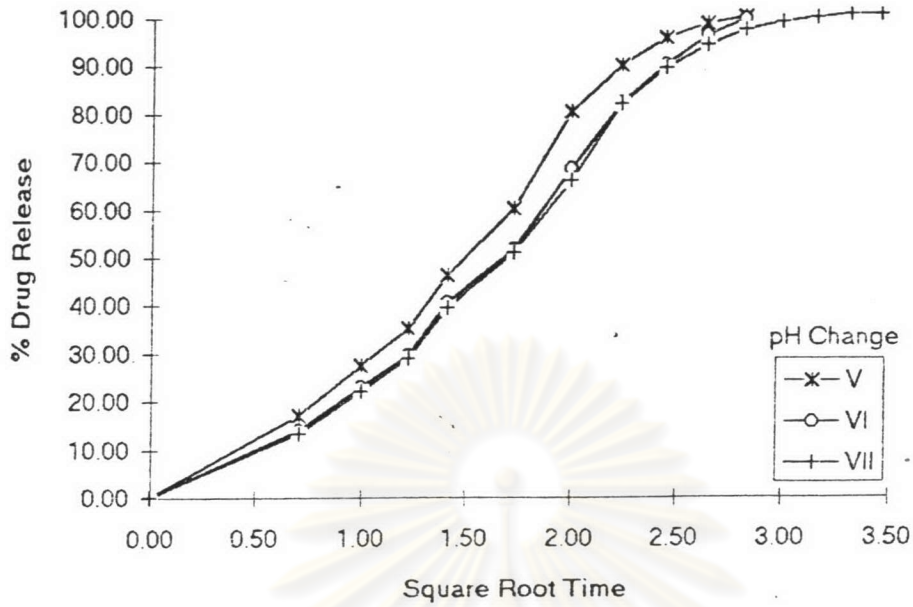


Figure 28 Higuchi plot of propranolol HCl-chitosan-HPMC matrices in pH change method

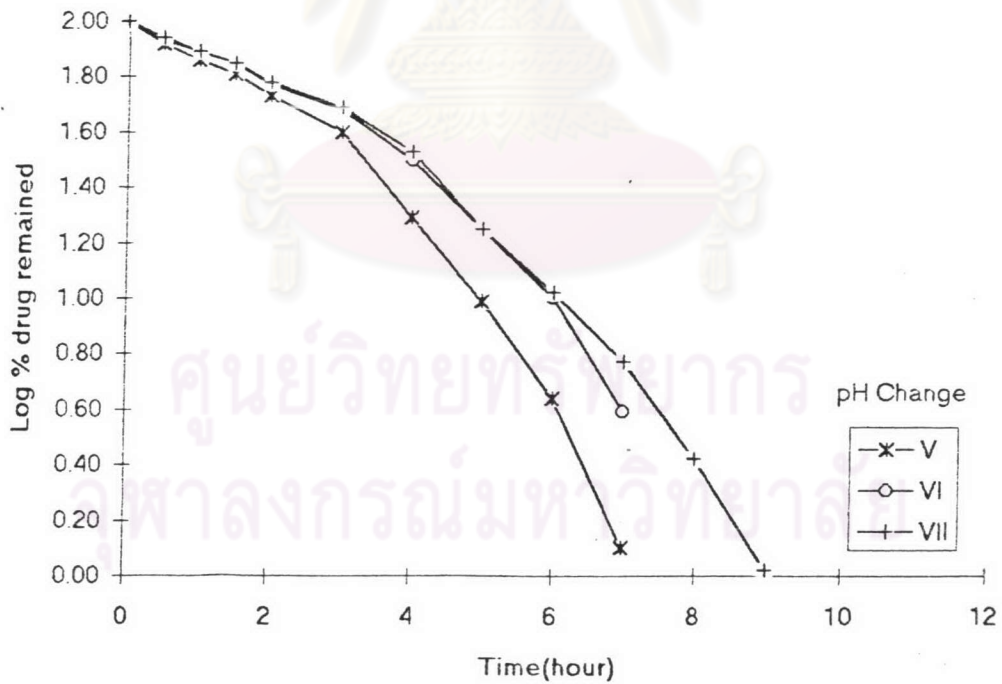


Figure 29 First-order plot of propranolol HCl-chitosan-HPMC matrices in pH change method

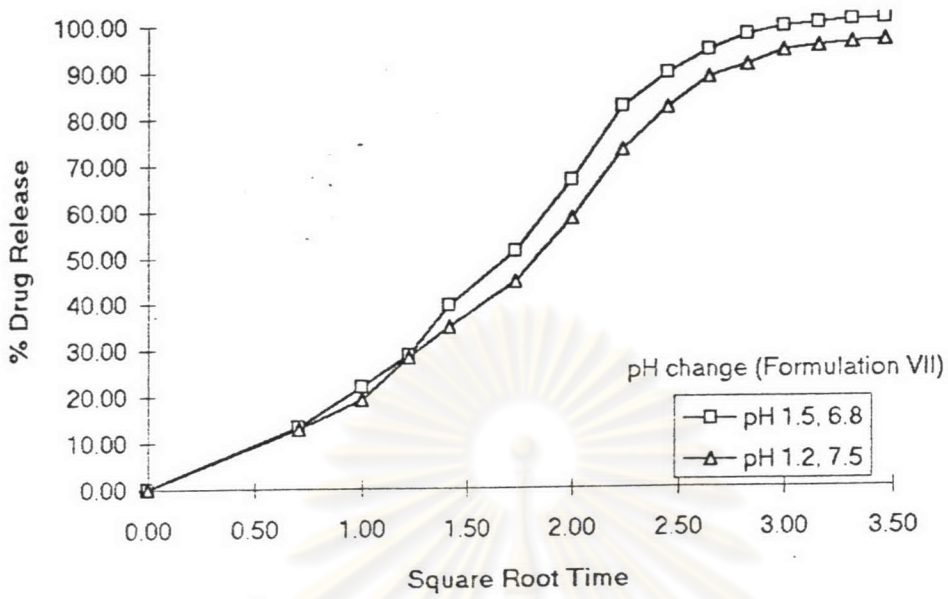


Figure 30 Higuchi plot of Formulation VII

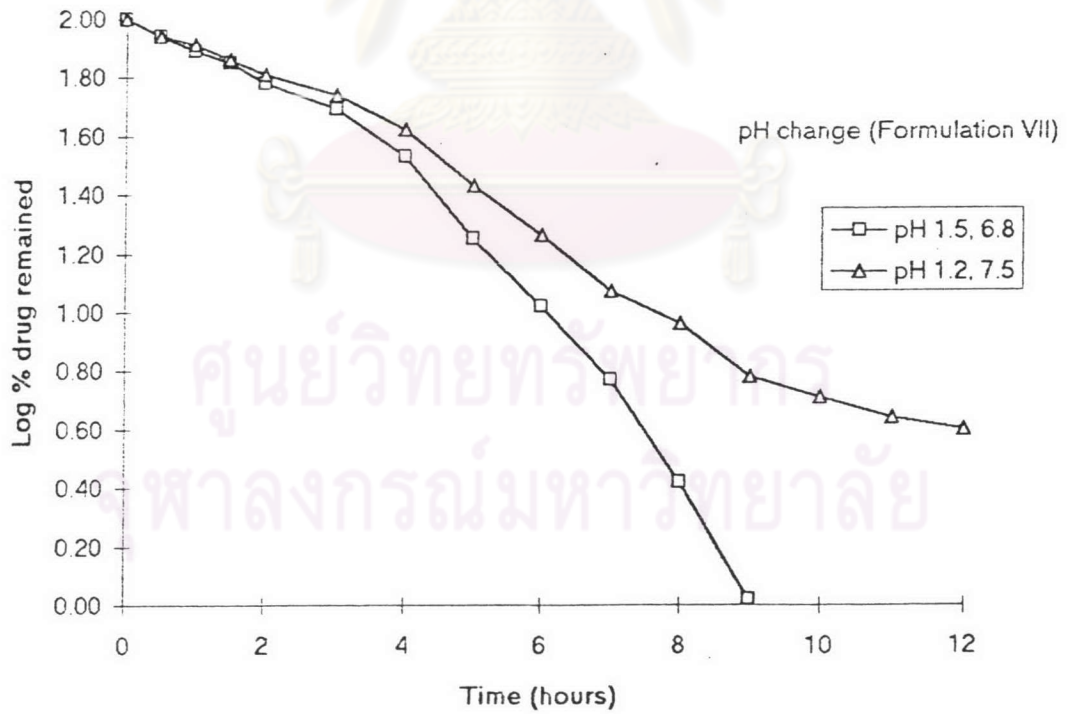


Figure 31 First-order plot of Formulation VII